Russian Journal of Biomechanics, Vol. 4, № 3: **-**, 2000

EXPERIMENTAL AND NUMERICAL ANALYSES OF WHIPLASH MOTIONS IN LOW-SPEED REAR-END COLLISIONS

H. Yoshida, S. Tsutsumi

Department of Medical Simulation Engineering, Institute for Frontier Medical Sciences, Kyoto University, 53 Kawahara-cho Shogoin Sakyo-ku, Kyoto 606-8507, Japan, e-mail: yoshida@frontier.kyoto-u.ac.jp

Abstract: Whiplash injuries occur frequently in rear-end car accidents even at low speed. In order to investigate the mechanism of whiplash injuries, experimental and finite element method (FEM) analyses were conducted. The Hybrid III dummy has been used for various experimental tests. However, since this dummy's neck is too rigid for low-speed collisions, we developed a new flexible neck model for low-speed rear-end collisions. In the experimental analysis using the new flexible neck model, the new neck model was more flexible than the Hybrid Ⅲ dummy neck model, and the displacement of the second cervical vertebra of the new flexible neck model was different from the others at 5 km/h. Higher compressive stress appeared in the soft tissues around the third cervical vertebra at 5 km/h in the FEM analysis. Therefore, it is supposed that the region between the second and the third cervical vertebra would be the most vulnerable to whiplash injuries.

Key words: whiplash injury, new flexible neck model, low-speed rear-end collision

Introduction

In Japan, statistical data show that 50% of all car accident injuries are caused in rear-end accidents, and 90% of people in rear-end accidents suffer neck injuries [1, 2]. Neck injuries in rear-end accidents occur even at low-speed and are known as «Whiplash injuries». It has been reported that these neck injuries occur in 40% of persons who sustain rear-end accidents even at low speeds of 5 km/h [1, 2].

Although various researchers have attempted to clarify the mechanism of whiplash injuries, this mechanism is not yet wholly understood [3-11], partly because research tests cannot reproduce actual rear-end car accidents. The Hybrid Ⅲ dummy (GM Ltd.) has typically been used internationally in experimental analyses. However, it is too rigid to analyze the whiplash motions in low-speed collisions because the Hybrid Ⅲ dummy neck model is made of aluminum plates and hard rubber, and is developed for frontal impact tests at high speed. Therefore, we developed a new neck model, which is more flexible than the Hybrid Ⅲ dummy neck model. In this study, we performed experimental analyses with the new flexible neck model to investigate the mechanism of whiplash motions. The results using the new flexible neck model were compared with those of the Hybrid Ⅲ dummy neck model.

However, it is impossible to observe internal stresses in experimental analyses with the new flexible neck model. Therefore, it is also valuable to carry out a computer numerical simulation. Thus, in this study, a numerical analysis was conducted using a finite element method (FEM). The FEM analysis was performed at low-speed rear-end collision to evaluate the deformation and the stress distributions after collision.

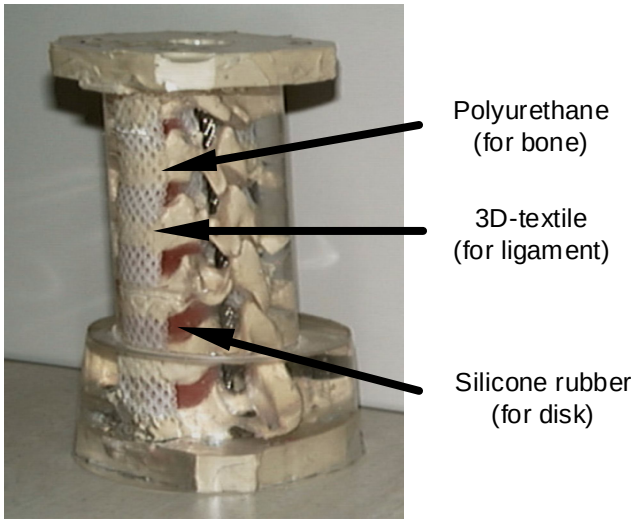

Fig. 1. New flexible neck model.

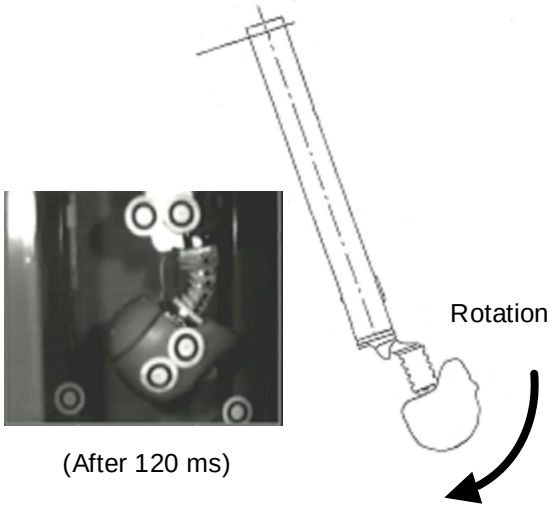

Fig. 2. Pendulum test.

Method

The new flexible neck model consisted of cervical vertebrae, ligaments, intervertebral disks, and soft tissues without muscles (Fig. 1) [4-7]. Since the response time of muscles by stimulus is reported to be as much as about 150ms to 250 ms after stimulus, the actions of the muscles could be disregarded during the analysis period up to 150ms in this study [12].

Each component of the new flexible neck model was made of many kinds of polymers having material properties close to those of the human body.

The cervical vertebrae were made of polyurethane and the first cervical vertebra was eliminated to make the length of the new neck model the same as that of the Hybrid Ⅲ dummy neck model. Thus, the number of cervical vertebrae was six. Ligaments were made of a 3-D (three-dimensional) textile (Cubic-eye HA6003, Unitika Co., Ltd.). The anterior longitudinal ligament had an elastic modulus of 6.6 MPa in the physiological range less than 5% [13, 14]. Tensile testing was performed and the result of Young's modulus of the 3-D textile was 3.7 MPa. Since the material properties of ligaments allow wide variations, we employed a 3-D textile for the ligaments. The 3-D textile has a nonlinear relation in tensile stress-strain action, which is peculiar to the behavior of the human soft tissues [15]. Five intervertebral disks were made of a silicone rubber (Dent silicone-V, Shofu Inc.). Young's modulus of the silicone rubber was 1 MPa or less from the results of tensile testing, and the annulus fibrosus of the intervertebral disk was 2 MPa [16]. In order to take the surrounding soft tissues of the human neck into consideration, the new flexible neck model was embedded in a transparent colorless silicone rubber (RTV Rubber KE1603, Shin-Etsu Chemical Co., Ltd.).

The response of the new flexible neck model was evaluated using a conventional Hybrid Ⅲ neck calibration pendulum test based on the rotation angle of the neck and the moment acting on the occipital condyle (Fig. 2) [4]. The new flexible neck model with the Hybrid Ⅲ dummy head was mounted on a rigid pendulum, and the pendulum was allowed to fall freely from a height at an impact speed of 5 km/h.

Experimental analysis was carried out to compare the behavior of the new flexible neck model with that of the Hybrid Ⅲ dummy neck model. These neck models were mounted on the Hybrid Ⅲ 50^{th} percentile male dummy. The Hybrid Ⅲ 50^{th} percentile dummy was seated on a frontal conventional seat for a small size car with and without a headrestraint in the sled tests (Fig. 3). The seatback angle was 22 degrees and the distance between the head and the

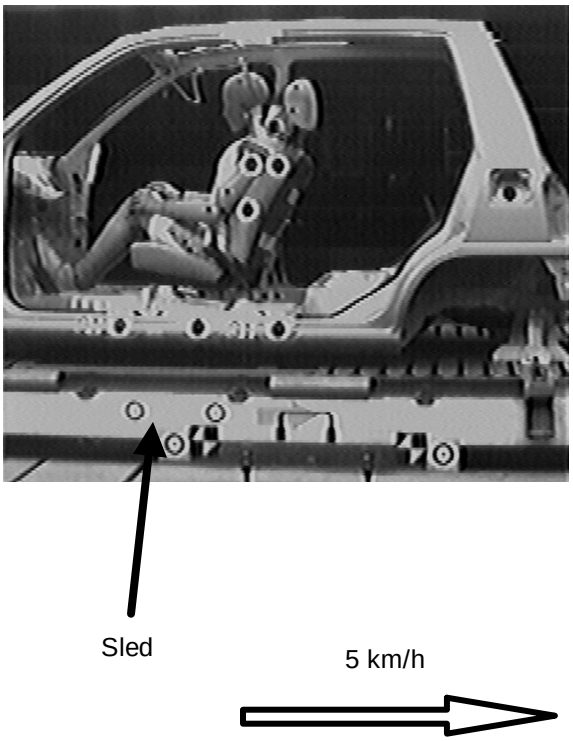

Fig. 3. Sled test.

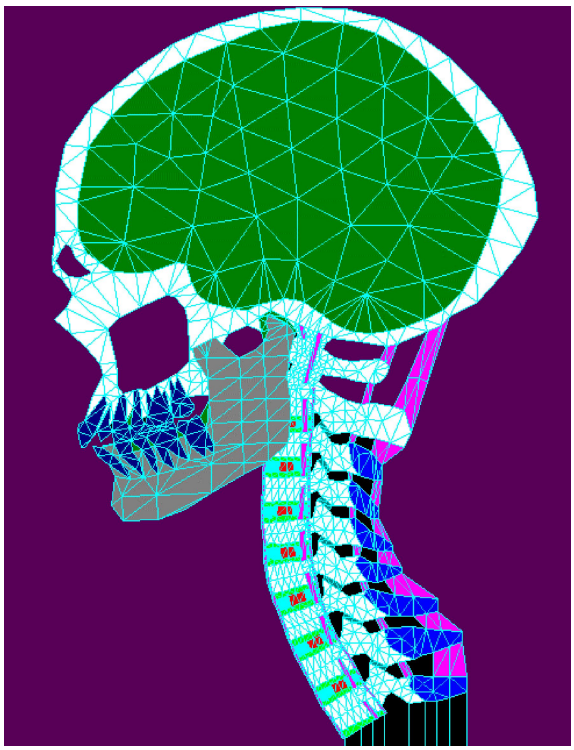

Fig. 4. FEM neck model.

headrestraint was set as 80 mm. The Hybrid Ⅲ dummy was restrained with a seat belt and the test speed was 5 km/h. Sled tests using the new flexible neck model were carried out and the initial seating posture of the Hybrid Ⅲ 50th percentile dummy was the same in all tests. The motions of two neck models were recorded with a high-speed video camera and this video system recorded one frame per one millisecond.

The FEM neck model was developed from X-ray photographs of a normal adult male and consisted of skull, cerebral cortex, cervical vertebrae (cortical bones, cancellous bones), thoracic vertebrae, ligaments, intervertebral disks (nucleus pulposus, annulus fibrosus) and soft tissues (Fig. 4). The FEM model was constructed as a pseudo 3-D neck model representing the head and neck down to the second thoracic vertebra. Thus, this FEM model consisted of three layers; the first layer included cancellous bones and intervertebral disks, the second layer included cortical bones, and the third layer included intertransverse ligaments.

The FEM analysis was conducted for the first 150 ms after collision and the restraint conditions were determined based on our sled test at 5 km/h (Fig. 5(a), (b)). Table 1 shows the material properties of each component. Since ligaments have a nonlinear relation in tensile stress-strain action, this property was introduced to ligaments of the FEM neck model. Analyses were carried out with Cosmos/M Ver.1.75 (SRAC Ltd.) on an IBM PC/AT compatible personal computer.

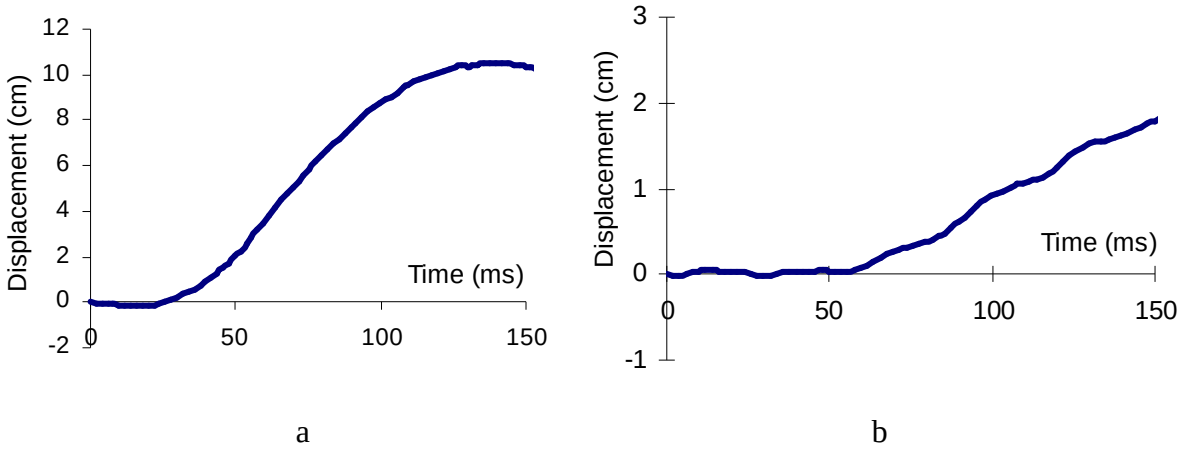

a b

Fig. 5: a – horizontal displacement of the second thoracic vertebra applied as an impact loading condition in FEM; b – upward displacement of the second thoracic vertebra applied as an impact loading condition in FEM.

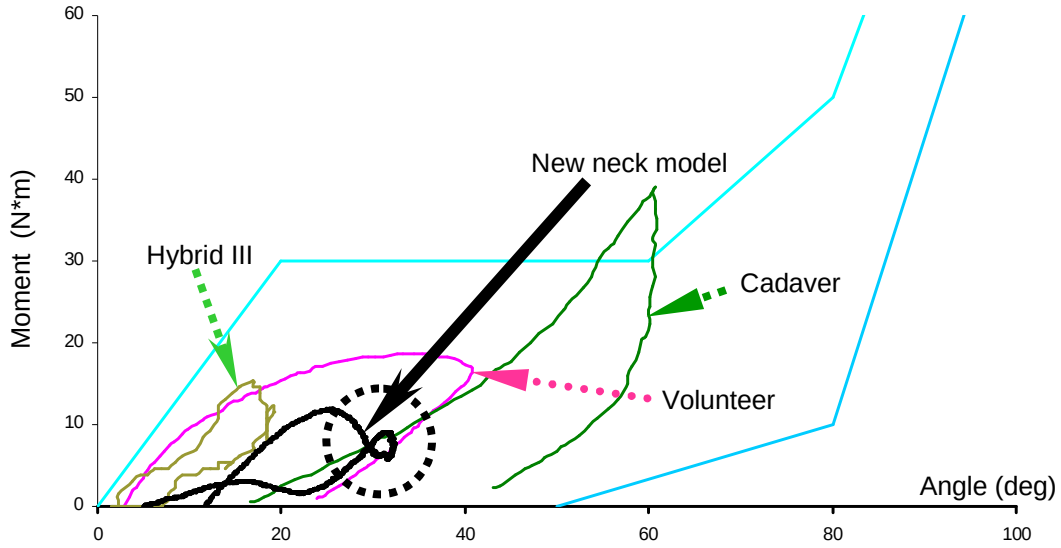

Fig. 6. Relation between rotation angle of neck and moment acting on occipital condyle in pendulum test.

Table 1. Material properties of FEM neck model.

Material	Young's modulus (MPa)	Poisson ratio
Cancellous bone	450	0.25
Intervertebral disk (annulus fibrosus)	5	0.4
Intervertebral disk (nucleus pulposus)	1	0.4
Ligament	10	0.3
Cortical bone	10000	0.29
Mandible	10000	0.25
Tooth	20000	0.25
Soft tissues	10	0.45

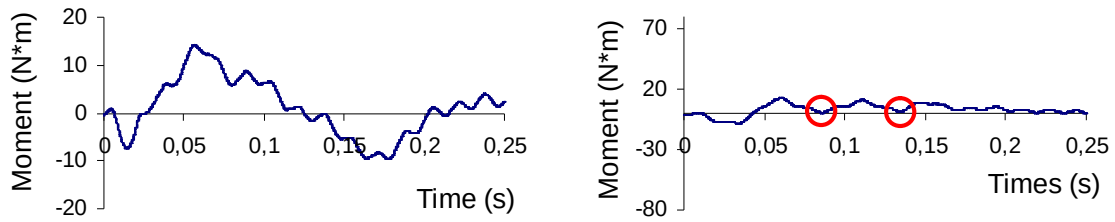

a b

Fig. 7: a – time vs. moment of dummy neck model in pendulum test; b – time vs. moment of new flexible neck model in pendulum test.

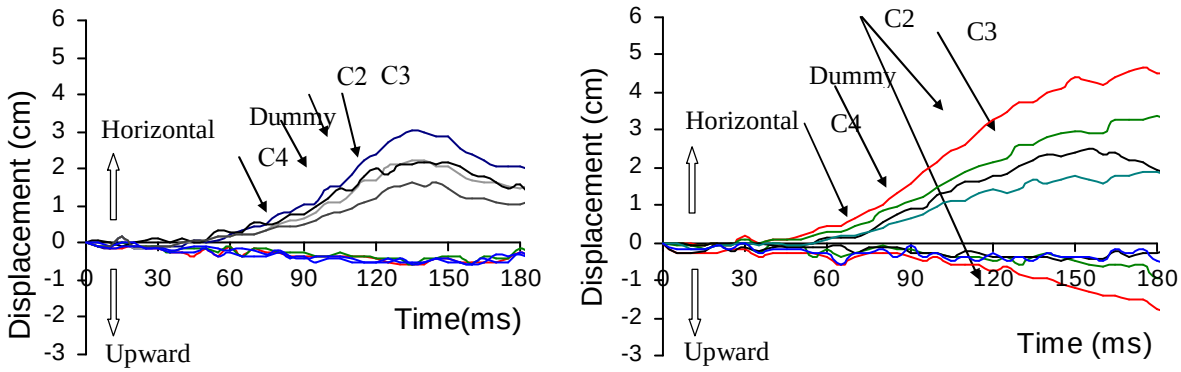

a b

Fig. 8: a – displacements with headrestraint in sled test (dummy: equivalent point to center between C2 and C3 of dummy neck); b – displacements without headrestraint in sled test.

Results and discussion

Figure 6 is a graph of the relationship between the rotation angle of the neck and the moment acting on the occipital condyle [4]. The X-axis shows the rotation angle and the Y-axis shows the moment. The curves representing the positions of the volunteer and cadaver were previously published data [4] and those of the new flexible neck model and the Hybrid Ⅲ dummy neck model were obtained from the results of our pendulum tests at 5 km/h.

The curve of the volunteer was located far to the left of the cadaver curve, which means that volunteers' necks were more rigid than cadaver's necks. It is assumed that this is because volunteers were already aware of the collision and they were thus subconsciously alert, so their necks were more rigid than real drivers' necks. Therefore, it is assumed that the curves of real drivers would be between the volunteer's curves and the cadaver neck curves. It is supposed that the motion of the new flexible neck model is more similar to that of real drivers in rear-end accidents because the curve of the new flexible neck model is presumed to be closer to the curve of the real drivers.

The shape of the curve of the new flexible neck model was different from the others in the pendulum test (Fig. 6). We attempted to consider this result from the relation between the time and the moment. Figures 7 (a) and (b) show the relationship between time and moment for the Hybrid Ⅲ dummy neck model and the new flexible neck model at 5 km/h, respectively.

The moment of the new neck model fell to zero at 80 ms while that of the dummy neck model did not fall. At 130 ms, the moment of the new neck model fell to zero again. From the result of the Hybrid Ⅲ dummy neck model in the pendulum test, the Hybrid Ⅲ

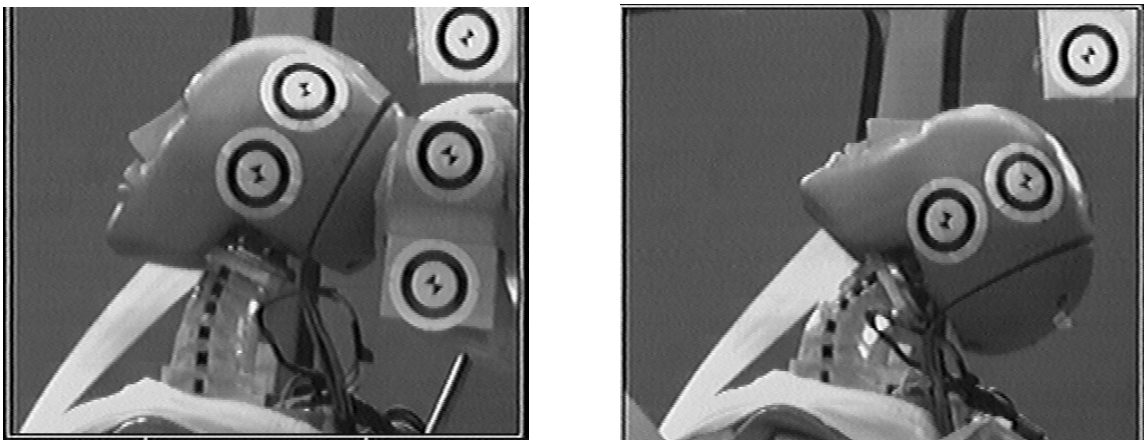

Fig. 9. Sled test with and without headrestraint after 150 ms.

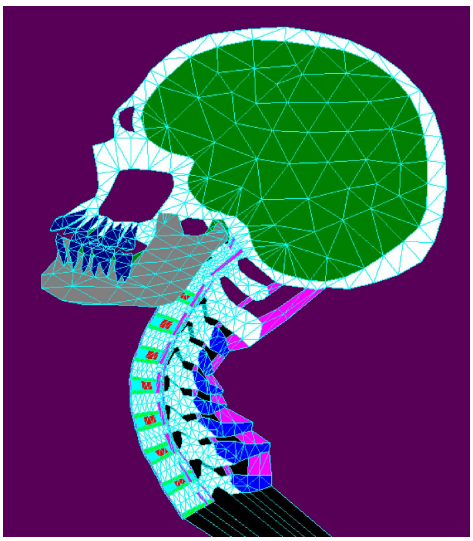

Fig. 10. Deformation of FEM neck model at 140 ms.

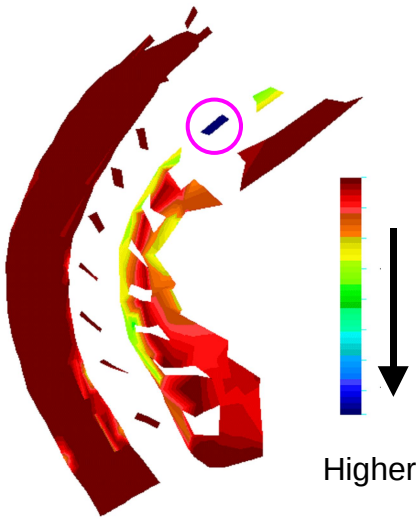

Fig. 11. Compressive stress at 140 ms (only soft tissues are illustrated).

dummy neck model did not rotate until 40 ms and the neck rotated backward up to 80 ms. After 80 ms, the dummy neck returned smoothly forward. In contrast, in the new flexible neck model, the neck rotated smoothly backward up to 80 ms. Since the neck bent around the third and the fourth cervical vertebrae at 80 ms, it was considered that the moment decreased. The neck continued to rotate backward until 120 ms and the moment fell to zero because shear displacement in the plane of the intervertebral disks appeared in the neck at 130 ms. The region within the dotted circle in Figure 6 is equivalent to the period from 80 ms to 130 ms in Figure 7 (b). Therefore, due to the difference in behavior during the period from 80 ms to 130 ms, the shape of the curve of the new flexible neck model was different from the others. It is supposed that this difference was caused by the flexibility of the new neck model; the 3-D textile of the new flexible neck model connects each cervical vertebra and each cervical vertebra can move separately and freely to some extent. However, the Hybrid Ⅲ dummy neck model consists of three plates of aluminum, hard rubber and a single steel cable, which exists through the center of the dummy neck model, and thus the parts do not move separately.

The results of the displacements of the cervical vertebrae of the new flexible neck model in the sled test are shown in Figures 8 (a) and (b). These are graphs of the displacement

of each cervical vertebra to the torso with and without the headrestraint. The positive direction of the Y-axis indicates the posterior displacement of the neck and a negative direction in the Y-axis shows an upward direction. Origin (0 ms) is the time when the sled was collided. Figure 9 gives photographs of the new flexible model with and without the headrestraint in the sled test at 150 ms after collision.

The displacements of the new flexible neck model were wholly larger than those of the Hybrid Ⅲ dummy neck. The new flexible neck model began to rotate at 50 ms and was restrained at 105 ms with the headrestraint. In the upward direction without the headrestraint, the displacement of the second cervical vertebra began to deviate from the others after 110 ms. The behavior of the new flexible neck model after collision was as follows; the torso was pushed to the seat back by the impact and then the torso moved forward by the reaction force of the seat back while the head remained in position due to inertia. After 100 ms, the torso continued to move forward while the head was rotating backward.

The FEM analysis showed that the head remained in position until about 100 ms after collision. The head remained in position due to inertia while the torso was abruptly moved forward. Subsequently, the neck was extended and it is considered that tensile stresses were generated. After 100 ms, the head began to rotate backward and the neck was significantly flexed around the third cervical vertebra (Fig. 10). When the shock wave reached to the head, the neck was compressed by the head and the highest compressive stress was observed in the soft tissues around the third cervical vertebra at 140 ms after collisions (Fig. 11). There is a possibility that the soft tissues around the second and third cervical vertebra would be damaged by this stress at about 140 ms. In the experimental analysis of the sled test, the displacement of the second cervical vertebra was different from the others. Therefore, this experimental result agrees well with the FEM result of the highest compressive stress at 140 ms.

Svensson reported that the head moves rearwards relative to the torso without any angular motion during the first phase, the linear rearward motion of the head is decelerated at the same time as the head starts rotating backward in the next phase, and the whole cervical spine goes into full extension in the last phase [8-9]. In our FEM analysis, the head remained in position and the neck was extended until about 100 ms, and the head began to rotate backward after 100 ms. Therefore, our FEM result was similar to the results of Svensson's report.

In the experimental analysis in the sled test, the displacement of the second cervical vertebra was different from the others. Stress concentration was observed in the soft tissues around the third cervical vertebra at 140 ms after collision in the FFM analysis. Therefore, it can be concluded that the region between the second and the third cervical vertebra is the most vulnerable to whiplash injuries.

According to the statistics of critical regions of whiplash injuries in rear-end accidents, the regions of injury symptoms are generally classified into two parts; the region including the upper cervical vertebrae (C2/3) and the region of the lower cervical vertebrae (C5/6/7) [17]. In this study, it was supposed that the region between the second and the third cervical vertebra, i.e. the upper cervical vertebrae, is the most vulnerable to whiplash injuries. Therefore, the results of this study agree well with the statistics.

Conclusions

Experimental and FEM analyses were carried out to investigate the mechanism of whiplash injuries.

In the experimental analysis using the new flexible neck model, the new neck model was more flexible than the Hybrid Ⅲ dummy neck model, and the displacement of the second cervical vertebra of the new flexible neck model was different from the others at 5 km/h.

In the FEM analysis, the highest compressive stress appeared in the soft tissues around the third cervical vertebra at 5 km/h. This FEM result agrees well with the results of the experimental analysis of the sled test.

Therefore, it is thought that the region between the second and the third cervical vertebra is the most vulnerable to whiplash injuries.

Acknowledgments

The authors wish to express their special thanks to the staff of Daihatsu Motor Co., Ltd. for providing the test devices and information.

References

1. Japan Automobile Research Institute, Inc., Research of a traffic accident, 1986, 1992 (in Japanese).
2. Japan Traffic Safety Association, **Traffic Green paper**, 1997 (in Japanese).
3. SHIMAMOTO N., TANAKA M., TSUTSUMI S., YOSHIDA H., MIYAJIMA Y. Developing Experimental Cervical Dummy Models for Testing Low-speed Rear-end Collisions. Enhanced Safety of Vehicles, 16th ESV Conf, paper NO. 98-S9-O-10, 1998.
4. MERTZ H, PATRICK L. Strength and Response of the Human Neck, **SAE** Paper No. 710855, 1971.
5. TSUTSUMI S., YOSHIDA H., MIYAJIMA Y. Impact Analysis of Whiplash Neck Behaviors in Rear-end Collisions. **Transactions of Jpn Soc Mech Eng**. 63: 791-796, 1997.
6. YOSHIDA H., MIYAJIMA Y., TSUTSUMI S. Numerical and Experimental Impact Analyses of Neck Behaviors in Rear-end Collisions. International Conf. New Frontier Biomech. Eng: 277-280, 1997.
7. YOSHIDA H., MIYAJIMA Y., TSUTSUMI S. Impacts Analyses of Whiplash Injuries in Rear-end Accidents. **J Jpn Soc Clin Biomech Related Res**, 18: 203-207, 1997 (in Japanese).
8. SVENSSON M.Y., ALDMAN B., HANSSON H.A., etc. Pressure Effects in the Spinal Canal During Whiplash Extension Motion: a Possible Cause of Injury to the Cervical Spinal Ganglia, **SAE** paper NO. 1993-13-0013, 189-200, 1993.
9. SVENSSON M.Y., etc. A Dummy for Rear-end Collisions: Development and Validation of a New Dummy-neck, **SAE** paper NO. 1992-13-0024, 299-310, 1992.
10. DENG Y.-C. Anthropomorphic Dummy Neck Modeling and Injury Considerations **Accid Anal Prev**, 21: 85-100, 1989.
11. SEEMANN M.R., MUZZY W.H., LUSTICK L.S. Comparison of Human and Hybrid Ⅲ Head and Neck Response. **STAPP Car Crash Conf**, Paper NO. 861892, 1986.
12. INOKAI M. **Guide of Physiology**. Kyorin shoin, 1963 (in Japanese).
13. AKAISHI F. Biomechanical Study of the Anterior and Posterior Longitudinal Ligaments in the Lower Cervical Spine. **J Jpn Soc Clin Biomech Related Res**, 15: 109-112, 1994 (in Japanese).
14. NOYES F.R. Functional Properties of Knee Ligaments and Alternations Induced by Immobilization. **Clin Orthop**, 123: 210-242, 1977.
15. YAMAGUCHI T. Study on the Strength of Human Skin. **J Kyoto Prefectural Univ Med**, 67: 347-379, 1960 (in Japanese).
16. TOTORIBE K. Biomechanical Study of The Lumbar Spondylolysis Using a Three-dimensional Finite Element Method and 3D-CT. **J Jpn Soc Clin Biomech Related Res**, 15: 99-102, 1994 (in Japanese).
17. SUGIMOTO T. **Whiplash Injury**, Nagai Shoten, 1972 (in Japanese).

Russian Journal of Biomechanics, Vol. 4, № 3: **-**, 2000

ЭКСПЕРИМЕНТАЛЬНЫЙ И ЧИСЛЕННЫЙ АНАЛИЗ ДВИЖЕНИЙ ПРИ “УДАРЕ ХЛЫСТОМ”, ВОЗНИКАЮЩИМ ПРИ УДАРЕ СЗАДИ В СЛУЧАЕ АВАРИЙ АВТОМОБИЛЕЙ С МАЛОЙ СКОРОСТЬЮ

Х. Иосида, С. Цуцуми (Киото, Япония)

Термином “удар хлыстом” называют удар, возникающий при ударе сзади по шее в случае столкновения автомобилей с малой скоростью (до 5 км/час). Статистика показывает, что в Японии 50 % всех травм при дорожно-транспортных происшествиях вызваны ударом сзади и 90 % потерпевших в этом случае получают травмы шеи. Несмотря на многие работы в этом направлении, механизм травм недостаточно понят. Это в значительной степени связано с тем, что в опытах не удается воспроизвести реальную ситуацию. Применяемые модели человека, сделанные из алюминиевых пластин и жесткой резины, имеют слишком большую жесткость.

В данной работе предложена и изготовлена новая конструкция модели, имеющая меньшую жесткость. Новая модель содержит шейные позвонки, связки, межпозвонковые диски и мягкие ткани без мышц. Последнее связано с тем, что действие мышц, как показывает опыт, проявляется через 150-250 миллисекунд после поступления импульса, а продолжительность удара меньше 150 миллисекунд. Описаны материалы, из которых сделаны новые элементы модели. Произведено сравнение результатов по перемещениям и моментам для обеих моделей при ударе с помощью калибровочного маятника. Исследована динамика перемещений и моментов для обеих моделей. Анализируется разница результатов измерений.

Расчет напряжений и перемещений произведен с помощью метода конечных элементов, причем проанализирована динамика изменений в течение 150 миллисекунд после удара. В модель входят череп человека, шейные позвонки (кортикальная и трабекулярная костные ткани), грудные позвонки, связки, межпозвонковые диски (пульповое ядро, фиброзное кольцо) и мягкие ткани. Применялся псевдотрехмерный метод расчета, при этом модель состояла из трех слоев.

Проведенные расчет и эксперимент позволили исследовать механизм травмы при “ударе хлыстом”. Анализируются повороты головы и изгибающие моменты в зависимости от времени после удара, причем расчет и новая экспериментальная модель дают близкие результаты.

Показано, что наиболее опасная область тела при данной травме сосредоточена между вторым и третьим шейными позвонками. Библ. 17.

Ключевые слова: травма при “ударе хлыстом”, новая экспериментальная модель, шея человека, удар сзади, столкновения автомобилей, эксперимент, метод конечных элементов

Received 10 May 2000